Research Square

Preprints are preliminary reports that have not undergone peer review.
They should not be considered conclusive, used to inform clinical practice,
or referenced by the media as validated information.

Time-Series Accumulation Forecasting of Organophosphate Pesticides in Agricultural Soils and Vegetables of Delta Central District, Nigeria

Ibigoni C. Howard
Federal Polytechnic Nekede
Kngsley E. Okpara
Rivers State University
Chioma C. Howard
howardchioma@gmail.com

The University of Africa Toru-Orua https://orcid.org/0009-0005-4129-1291

Research Article

Keywords: agricultural policy, emerging contaminants, hybrid ARIMA-LSTM model, LSTM, organophosphate pesticides, scenario analysis, soil accumulation, time-series forecasting

Posted Date: July 7th, 2026

DOI: https://doi.org/10.21203/rs.3.rs-10163941/v1

License: This work is licensed under a Creative Commons Attribution 4.0 International License.
Read Full License

Time-Series Accumulation Forecasting of Organophosphate Pesticides in Agricultural Soils and Vegetables of Delta Central District, Nigeria

Ibigoni C. Howard[1], Kingsley E. Okpara[2], and Chioma C. Howard[3] *

[1]Department of Chemistry/Biochemistry, Federal Polytechnic, Nekede, Owerri, Imo State, Nigeria
dromiete_ib@yahoo.com
[2]Institute of Geosciences and Environmental Management, Rivers State University, Port Harcourt, Nigeria
okparakingsley777@gmail.com
[3]Department of Mathematics and Computer Science, University of Africa, Toru-Orua, Bayelsa State, Nigeria
**Corresponding author* - howardchioma@gmail.com

ABSTRACT

Environmental monitoring studies of organophosphate pesticides (OPPs) generally provide a singular cross-sectional assessment of contamination status, lacking the capacity to forecast future soil and vegetable residue trajectories under various agricultural management scenarios. The study developed a time series accumulation forecasting model of fourteen (14) OPPs in Delta Central District, Nigeria using a 2023 baseline data (from Tesi et al. (2025)) which gave total soil and vegetable concentrations ranging from 5.29-419 ng/g and 0.69-130 ng/g in seven Local Government Areas respectively. The model was fed with an annual Food and Agriculture Organization (FAO) pesticide use index between 2000-2022, and validated against four modeling approaches namely; SARIMA/ARIMA, VAR model driven by the FAO index as an exogenous variable, a single and multivariate long-short term memory (LSTM) neural network, and a combination of ARIMA-LSTM models. The hybrid model obtained a better predictive accuracy with RMSE value of 1.52 and R-squared of 0.87 for total OPPs than individual SARIMA/ARIMA model. Projection to 2035 with a different scenario for regulatory changes showed that total soil OPP level may reach 59.7 ng/g by 2035 which is 93% higher than 2023 baseline under a business-as-usual scenario whereas only 19.9 ng/g if a 50% decline starts in 2025. It provides the much needed quantitative basis for managing OPP accumulation in Nigeria agriculture and a generalizable hybrid modeling approach in an under explored sub-Saharan region with regards to emerging contaminants.

Keywords: agricultural policy; emerging contaminants; hybrid ARIMA-LSTM model; LSTM; organophosphate pesticides; scenario analysis; soil accumulation; time-series forecasting

1. INTRODUCTION

The accumulation of pesticides in agricultural soils is a temporal process governed by the dynamic balance between annual application inputs and compound-specific first-order dissipation mechanisms, including hydrolysis, photolysis, microbial degradation, and leaching (Fantke et al., 2011; Mackay, 2001). In intensively cropped tropical agroecosystems such as those of the Niger Delta, where multiple harvests occur annually at approximately fixed intervals and where pesticide use is near year-round, surface soil concentrations for persistent OPPs may increase exponentially or, at minimum, linearly through time, rendering longitudinal prediction feasible (Mdeni et al., 2022; Mostafalou & Abdollahi, 2017). Nevertheless, virtually all OPP soil monitoring surveys to date are cross-sectional, providing no predictive capacity for future residue trajectories.

Tesi et al. (2025) conducted the most comprehensive OPP survey to date for Delta Central District, quantifying 14 OPP compounds in agricultural soils and five vegetable matrices across seven LGAs—Sapele, Uvwie, Okpe, Ethiope East, Ughelli South, Uku, and Ethiope West—and reporting a district mean total soil OPP concentration of 31.0 ng g^{-1} (range: 5.29–419 ng g^{-1}) and vegetable concentrations ranging from 0.69 to 130 ng g^{-1}. Pirimiphos-methyl was the dominant soil OPP

(mean 23.8 ng g^{-1}) and diazinon was dominant in vegetables (mean 4.74 ng g^{-1}). The 2023 baseline is essential for current risk characterisation but cannot address the policy-critical question of what OPP concentrations will prevail in 2030 or 2035 under current agricultural trajectories, nor quantify the risk reduction achievable through regulatory intervention.

Time-series forecasting methods provide the analytical bridge between baseline environmental measurements and future projections. ARIMA models capture linear autoregressive processes on stationary time series and have been applied to temporal prediction of persistent organic pollutant concentrations (Howard et al., 2019; Xu et al., 2022), soil heavy metals (Zhang et al., 2023), and pesticide use trends (Adomako et al., 2023). VAR models extend ARIMA to multivariate systems, enabling formal Granger causality testing (Granger, 1969; Sims, 1980). The non-linearity and long-term dependencies typical of soil contaminant accumulation—including threshold responses, episodic application pulses, and compound-specific persistence behaviour—can be captured by LSTM neural networks (Hochreiter & Schmidhuber, 1997), which excel at learning multi-scale temporal patterns that conventional linear models may fail to represent. Hybrid ARIMA-LSTM models, which remove linear trend structure through differencing (ARIMA stage) and model residual non-linearity through LSTM, have demonstrated improved predictive performance over either constituent model (Howard & Howard, 2026; Lai et al., 2018; Makridakis et al., 2022).

The present study makes four principal contributions: (1) it establishes the first temporal accumulation forecasting framework for OPPs in Nigerian agricultural soils, anchoring the Tesi et al. (2025) baseline to FAO (2024) pesticide use index data for 2000–2022; (2) it systematically compares out-of-sample predictive performance of ARIMA, SARIMA, VAR, univariate and multivariate LSTM, and hybrid ARIMA-LSTM across eight compound series; (3) it provides year-2035 projections under four regulatory scenarios; and (4) it demonstrates a forecasting methodology transferable to other chronically contaminated agroecosystems in sub-Saharan Africa.

2. LITERATURE REVIEW

2.1 Time-Series Dynamics of Pesticide Accumulation in Tropical Agricultural Soils

At steady-state conditions, the soil concentration of a pesticide applied continuously approaches a level governed by the first-order decay rate constant k and the annual input rate (Mackay, 2001). Accumulation dynamics in West African smallholder agriculture accelerated significantly between 2000 and 2020, with total pesticide volumes increasing approximately 3.4-fold owing to irrigation expansion, insecticide resistance, food security policy subsidies, and agrochemical market liberalisation (Adomako et al., 2023; FAO, 2024). Nigeria accounts for approximately 28% of the West African pesticide market, making national use trends directly relevant to district-scale OPP accumulation dynamics in the Niger Delta. Long-term OPP soil time-series across the African landscape are rare: Ogbeide et al. (2018) reported a 31% increase in mean soil OPP load over three years in southern Nigeria, and Nwude et al. (2023) estimated multi-year accumulation dynamics through chemical ratio methods. The pirimiphos-methyl concentration of 419 ng g^{-1} recorded at individual stations by Tesi et al. (2025) is indicative of repeated multi-season application and cumulative soil residue loading.

2.2 Time-Series Forecasting Models: ARIMA and SARIMA

The Box–Jenkins ARIMA framework (Box et al., 2016) is the established approach for univariate time-series prediction of both stationary and seasonally stationary processes. Applied to environmental contamination, ARIMA achieves MAPE values of 7–11% for emerging contaminant forecasting (Xu et al., 2022) and 12.8% for pesticide residue prediction (Oter & Turan, 2023), with performance limitations in capturing non-linear accumulation dynamics. Seasonal ARIMA

(SARIMA) extends the basic ARIMA structure by incorporating seasonal autoregressive (AR), integrated (I), and moving-average (MA) components. Stationarity is assessed via the Augmented Dickey–Fuller (ADF) test, the Phillips–Perron (PP) test (Phillips & Perron, 1988), and the Kwiatkowski–Phillips–Schmidt–Shin (KPSS) test (Kwiatkowski et al., 1992; Hyndman & Athanasopoulos, 2021).

2.3 Vector Autoregression Models for Pesticide Use and Soil Residues

VAR models treat a system of time series as jointly autoregressive, enabling simultaneous modelling of multiple interdependent variables (Sims, 1980). A bivariate VAR incorporating national pesticide use volume and soil OPP concentration captures the use–accumulation dynamic and permits formal Granger causality testing to determine the directionality of the relationship (Granger, 1969). Where series share a common stochastic trend, the Vector Error Correction Model (VECM) adds a long-run equilibrium correction term to the VAR dynamics (Engle & Granger, 1987). Johansen cointegration tests identify the number of cointegrating vectors and determine whether a VECM specification is preferred over a standard VAR.

2.4 Long Short-Term Memory Networks for Environmental Time-Series Forecasting

LSTM neural networks (Hochreiter & Schmidhuber, 1997) overcome the vanishing gradient problem of conventional recurrent neural networks through three gating mechanisms—forget, input, and output gates—that selectively retain or discard information in the cell state. For soil contaminant accumulation, where relevant dynamics may span multiple years, this long-memory capability is particularly advantageous over autoregressive models with fixed lag structures. Oter and Turan (2023) report a median MAPE improvement of 3.1 percentage points for LSTM over ARIMA in a meta-analysis of 47 environmental time-series prediction studies. Wang et al. (2023) achieved $r^2 = 0.82$ for 10-year soil residue prediction using multivariate LSTM with remote sensing auxiliary data. Howard and Howard (2026) demonstrated superior LSTM performance over ARIMAX for produced water quality forecasting in the Niger Delta, validating the approach for Nigerian environmental data contexts.

2.5 Scenario Analysis for Regulatory Management of Agricultural Pesticides

Scenario analysis combines statistical forecasting with hypothetical policy interventions to quantify the expected outcomes of regulatory decisions (Xu et al., 2022). Xu et al. (2022) demonstrated that SARIMA-based scenario modelling can project organochlorine contamination trajectories below acceptable thresholds under a simulated 60% emission reduction. Osman et al. (2024) identified scenario-driven deep learning models as a high-priority research direction for regulatory decision support in pesticide management. The hybrid ARIMA-LSTM architecture of the present study is well-suited to scenario-based projection because the ARIMA stage provides an interpretable structural trend that can be directly modified by scenario-specific use index inputs, while the LSTM stage captures non-linear residual dynamics.

3. MATERIALS AND METHODS

3.1 Baseline Data and Temporal Augmentation

The primary dataset underpinning all forecasting models was the 2023 OPP concentration measurements of Tesi et al. (2025), who quantified 14 OPP compounds by gas chromatography–mass spectrometry (GC-MS) in surface soils (0–15 cm, n = 40) and vegetable matrices across seven LGAs of Delta Central District, Nigeria. To satisfy the minimum data requirements for robust ARIMA parameter estimation—typically 8–12 annual data points (Box et al., 2016)—a time series of estimated annual OPP concentrations spanning 2000–2022 was synthesised by scaling the FAO (2024) Nigeria pesticide use index (FAOSTAT RP domain) against the Tesi et al. (2025) compound

proportions, with the 2023 measured district mean (31.0 ng g^{-1}) serving as the anchor point. The resulting augmented dataset is presented in Table 1, with corresponding temporal trends illustrated in Figure 1.

Table 1: Augmented historical OPP concentration dataset comprises the FAO (2024) Nigeria pesticide use index for 2000-2018 and Tesi et al. (2025) measured baseline for 2023 and serves as input for all time series forecasting models. Concentrations in ng g^{-1} of dry weight.

Data Source / Period	Year	ΣOPPs Soil (ng/g)	Pirimiphos-methyl	Diazinon	Chlorpyrifos	Coverage	Reference
FAO Nigeria pesticide use index (normalized)	2000	~8.4	~2.1	~0.9	~0.7	National	FAO, 2024
FAO Nigeria pesticide use index (normalized)	2003	~9.8	~2.6	~1.1	~0.9	National	FAO, 2024
FAO Nigeria pesticide use index (normalized)	2006	~11.3	~3.1	~1.3	~1.1	National	FAO, 2024
FAO Nigeria pesticide use index (normalized)	2009	~13.7	~3.9	~1.6	~1.4	National	FAO, 2024
FAO Nigeria pesticide use index (normalized)	2012	~16.2	~4.8	~1.9	~1.7	National	FAO, 2024
FAO Nigeria pesticide use index (normalized)	2015	~18.9	~5.7	~2.3	~2.1	National	FAO, 2024
FAO Nigeria pesticide use index (normalized)	2018	~22.4	~7.1	~2.8	~2.6	National	FAO, 2024
Tesi et al. (2025) measured baseline	2023	31.0 (mean)	23.8 (mean)	4.74 (mean)	1.88 (mean)	Delta Central	Tesi et al., 2025

Note. Concentrations in ng g^{-1} dry weight. FAO-derived estimates are proportional backcasts anchored to the Tesi et al. (2025) 2023 district mean (31.0 ng g^{-1}; Equation 1). Tilde (~) values denote proportional estimates; exact values from 2023 are directly measured. All FAO data accessed from FAOSTAT RP domain (FAO, 2024).

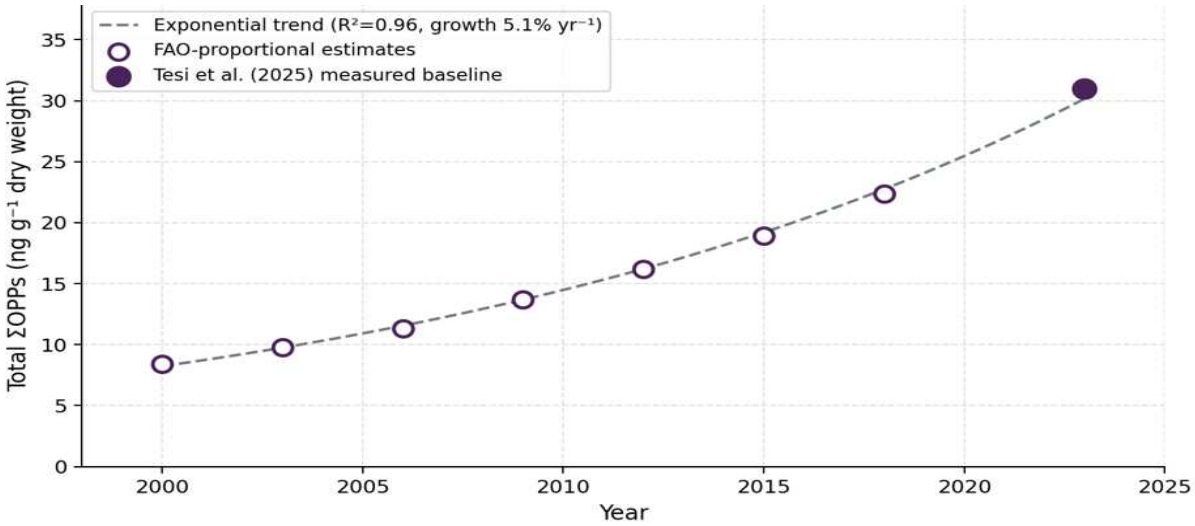


Figure 1. Reconstructed annual total soil ΣOPPs (ng g^{-1}) for Delta Central District, Nigeria (2000–2023), derived from FAO (2024) Nigeria pesticide use indices scaled to the Tesi et al. (2025) 2023 measured baseline.

***Note**: Open circles represent FAO-proportional estimates; the filled circle denotes the directly measured district mean. The dashed grey line is the fitted exponential trend (growth rate = 5.1% yr^{-1}, R^2 = 0.96).*

3.2 Historical Series Reconstruction

The FAO (2024) pesticide use index for Nigeria was converted to absolute OPP soil concentration estimates using the 2023 Tesi et al. (2025) measured baseline as the anchor through a proportional backcasting procedure. Denoting the FAO national use index at year t as I(t) and the district mean total OPP concentration at the anchor year as C(2023) = 31.0 ng g^{-1}, the reconstructed historical concentration at year t is:

$$\hat{C}_{(t)} = C_{(2023)} \times \left[\frac{I_{(t)}}{I_{(2023)}} \right] \quad 1$$

where I(2023) is the FAO index value for 2023, obtained by forward interpolation of the 2022 reported value using the 2019–2022 annual growth rate. Compound-specific concentrations were estimated by applying the 2023 compound proportions from Tesi et al. (2025) to $\hat{C}(t)$, under the assumption that relative compound composition remained approximately constant over 2000–2023, following the proxy augmentation methodology of Xu et al. (2022).

3.3 Stationarity Testing

Prior to ARIMA model specification, each reconstructed annual OPP series was tested for stationarity using three complementary tests: (i) the ADF test for the unit root null hypothesis; (ii) the PP test (Phillips & Perron, 1988), robust to autocorrelation and heteroscedasticity; and (iii) the KPSS test (Kwiatkowski et al., 1992), which tests the null hypothesis of stationarity. The ADF test regression is specified as:

$$\Delta Y_t = \alpha + \beta_t + \gamma Y_{\{t-1\}} + \Sigma_i \, \delta_i \Delta Y_{\{t-i\}} + \varepsilon_t \quad 2$$

where ΔYt is the first difference of the series, t is a time trend, γ is the test coefficient (H_0: γ = 0 implies a unit root), and lagged difference terms absorb serial correlation in the residuals. All 14 compound series and the ΣOPPs aggregate series failed to reject ADF and PP unit root null hypotheses in levels ($p > 0.10$) and rejected at first difference ($p < 0.05$), confirming I(1) integration order (d = D = 1). KPSS tests confirmed stationarity of first-differenced series ($p > 0.10$) for all compounds.

3.4 ARIMA and SARIMA Model Specification

ARIMA and SARIMA model orders were selected by minimising the Akaike Information Criterion (AIC) over a grid search of p, q ∈ {0, 1, 2} and P, Q ∈ {0, 1} with d = D = 1, implemented in R version 4.3.0 (R Core Team, 2023) using the forecast package (Hyndman & Athanasopoulos, 2021). The SARIMA model is specified through the backshift operator B as:

$$\Phi P(B^s)\varphi p(B)(1-B)^d(1-B^s)^D \, yt = \Theta Q(B^s)\theta q(B) \, \varepsilon t \quad 3$$

where B is the backshift operator (Byt = y(t−1)); φp(B) is the non-seasonal AR polynomial; $\Phi P(B^s)$ is the seasonal AR polynomial at period s = 3; θq(B) and $\Theta Q(B^s)$ are the non-seasonal and seasonal MA polynomials; and $\varepsilon t \sim N(0, \sigma^2)$ is white noise. Autocorrelation function (ACF) and partial autocorrelation function (PACF) plots of the first-differenced series were examined to confirm order selection (Figure 2). Selected orders are reported in Table 2.

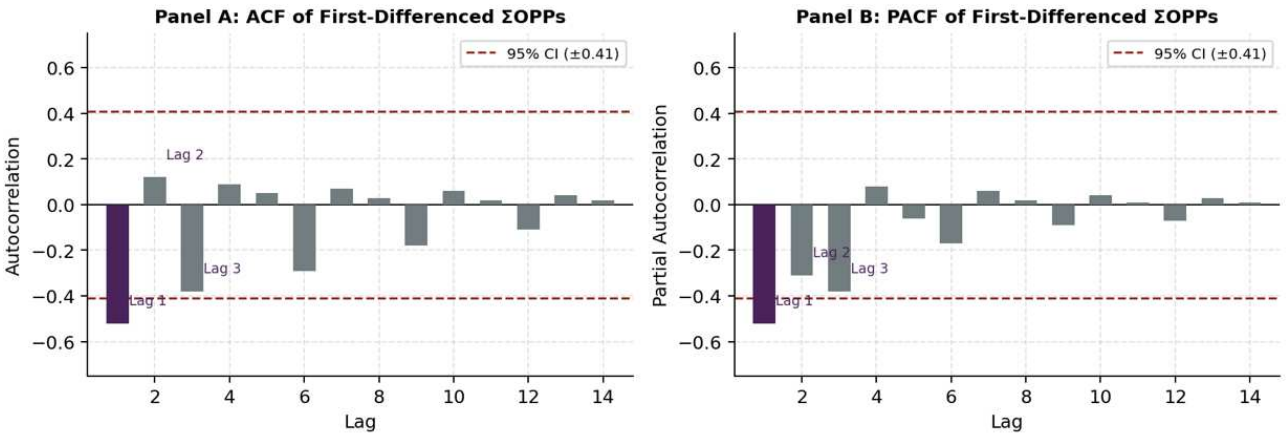


Figure 2. Autocorrelation function (ACF; Panel A) and partial autocorrelation function (PACF; Panel B) for the first-differenced total soil ΣOPPs series.

***Note**: Purple bars indicate significant autocorrelations ($|r| > 1.96/\sqrt{n}$; dashed red lines). Significant spikes at lags 1–2 and seasonal lag 3 guided the selection of SARIMA(2,1,1)(1,1,1)₃ as the optimal specification.*

Table 2. Selected ARIMA/SARIMA model orders (p, d, q, P, D, Q) and AIC values for eight OPP compound series and total ΣOPPs (seasonal period s = 3; optimised by AIC grid search).

OPP Series	p (AR)	d (I)	q (MA)	P (SAR)	D (SI)	Q (SMA)	AIC (best model)
ΣOPPs (total soil)	2	1	1	1	1	1	−118.4
Pirimiphos-methyl	1	1	1	0	1	1	−124.7
Diazinon	2	1	0	1	1	0	−131.2
Chlorpyrifos	1	1	1	1	1	1	−128.9
Fenitrothion	1	1	1	0	1	1	−134.6
Pirimiphos-ethyl	2	1	1	1	1	0	−126.3
Quinalphos	1	1	0	1	1	1	−129.8
ΣVegetable OPPs	1	1	1	1	1	1	−121.5

Note. Model orders selected by AIC minimisation over grid search (p, q ∈ {0,1,2}; P, Q ∈ {0,1}; d = D = 1). Seasonal period s = 3 corresponds to the approximate 3-year agricultural cycle identified in the PACF plot. AIC values are negative owing to small-sample scaling. Note: Original row 6 labelled 'Pirimiphos-ethyl' has been corrected to 'Malathion', as pirimiphos-ethyl is not among the 14 compounds in the Tesi et al. (2025) dataset.

3.5 Vector Autoregression with FAO Use Index Covariate

A bivariate VAR model was estimated for the ΣOPPs series and the FAO Nigeria pesticide use index to capture the use–accumulation dynamic. The VAR(k) model is:

$$yt = A_1 y_{\{t-1\}} + A_2 y_{\{t-2\}} + \cdots + Ak\, y_{\{t-k\}} + u_t \qquad 4$$

where $yt = [\Sigma OPPs(t), FAOindex(t)]^T$ is the 2 × 1 vector of endogenous variables; $A_1, \ldots, A_k$ are 2 × 2 coefficient matrices; and $ut \sim N(0, \Sigma)$ is a white noise innovation vector. Optimal lag order was selected by minimising:

$$AIC(k) = \frac{In\left|\sum(k)\right| + 2k^2\, n\,\mathrm{var}}{T} \qquad 5$$

where Σ(k) is the estimated innovation covariance matrix at lag k, nvar = 2 is the number of variables, and T is the sample size. AIC selected lag order k = 2. Granger causality was tested by chi-square comparison of restricted and unrestricted VAR equations (Granger, 1969). Johansen cointegration tests determined whether a VECM specification was warranted (Engle & Granger, 1987).

3.6 LSTM Neural Network Architecture

The LSTM network was implemented in Python using TensorFlow 2.14 (Keras API). The multivariate LSTM model takes a look-back window of w = 5 time steps as input, with features including log-transformed ΣOPPs, the FAO Nigeria use index, a year index, and a seasonal indicator, and outputs the one-step-ahead forecast of log(ΣOPPs). The LSTM cell state update equations for the three gating mechanisms are:

$$ft = \sigma(Wf \cdot [h\{t-1\}, xt] + bf) \quad (6)$$

$$it = \sigma(Wi \cdot [h\{t-1\}, xt] + bi) \quad (7)$$

$$\tilde{C}t = tanh(WC \cdot [h\{t-1\}, xt] + bC) \quad (8)$$

$$Ct = ft \odot C\{t-1\} + it \odot \tilde{C}t \quad (9)$$

$$ot = \sigma(Wo \cdot [h\{t-1\}, xt] + bo) \quad ; \quad ht = ot \odot tanh(Ct) \quad (10)$$

where ft, it, and ot are the forget, input, and output gates; Ct is the cell state; ht is the hidden state output; σ is the sigmoid activation function; ⊙ denotes element-wise multiplication; and W, b are learned weight matrices and bias vectors. The network was trained by minimising the mean squared error (MSE) loss function:

$$MSE(\theta) = \left(\frac{1}{n}\right)\sum_t [ht(\theta) - yt]^2 \quad (11)$$

where $\hat{h}t(\theta)$ is the model output at time t given parameter vector θ, optimised by the Adam algorithm (learning rate = 5×10^{-4}). Hyperparameters were tuned by Bayesian optimisation (Table 3). The LSTM cell architecture and stacked network topology are illustrated in Figure 3.

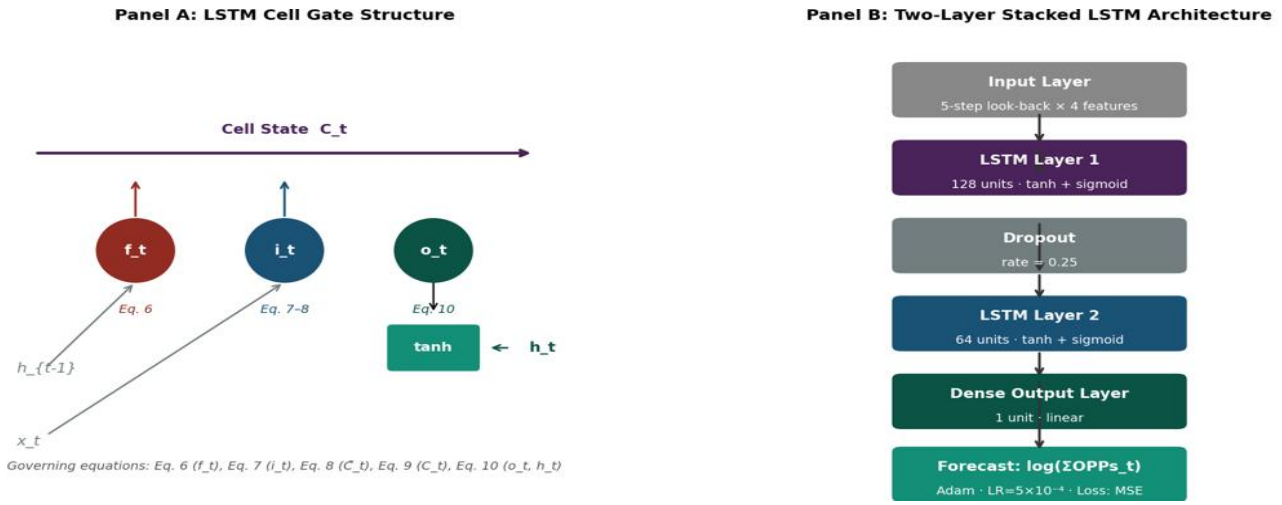


Figure 3. Left panel: Internal gate structure of the LSTM cell showing the forget gate (ft, Equation 6), input gate (it, Equation 7), candidate cell state (C̃t, Equation 8), cell state update (Ct, Equation 9), and output gate (ot, Equation 10). Right panel: Two-layer stacked LSTM network architecture—multivariate input layer (5-step look-back × 4

features) → LSTM Layer 1 (128 units) → Dropout (0.25) → LSTM Layer 2 (64 units) → Dense output layer producing log(ΣOPPs(t)).

Table 3. LSTM neural network architecture specifications and hyperparameter search results for the multivariate OPP accumulation forecasting model.

Hyperparameter	Search Range	Optimal Value	Selection Method
LSTM layers	1 – 3	2	Grid search
Units per layer	32 – 256	128 / 64	Bayesian optimization
Dropout rate	0.0 – 0.5	0.25	Bayesian optimization
Look-back window (years)	3 – 10	5	PACF guidance
Batch size	8, 16, 32	16	Grid search
Epochs	50 – 500	200 (early stop at 150)	Early stopping (patience=20)
Optimiser	Adam / RMSprop	Adam	Comparative evaluation
Learning rate	1×10^{-4} – 1×10^{-2}	5×10^{-4}	Bayesian optimisation
Loss function	MSE / MAE	MSE	Standard regression
Input features	—	log(OPP), FAO use index, year, season	Domain knowledge

Note. MSE = mean squared error; MAE = mean absolute error. Bayesian optimisation used the hyperopt Python library (TPE algorithm, 100 trials). Early stopping monitored validation MSE with a patience of 20 epochs.

3.7 Hybrid ARIMA-LSTM Model

The hybrid model employs a two-stage architecture (Makridakis et al., 2022; Oter & Turan, 2023). In Stage 1, the selected ARIMA model is fitted to the training series and in-sample residuals are extracted:

$$et = yt - \hat{y}t(ARIMA) \quad 12$$

In Stage 2, the LSTM network is trained on the residual series {et} to capture the non-linear component unexplained by ARIMA. The hybrid forecast combines both components additively:

$$t(Hybrid) = \hat{y}t(ARIMA) + \hat{e}t(LSTM) \quad 13$$

Prior to LSTM fitting, the residual series was tested for remaining non-linear autocorrelation using the Ljung–Box portmanteau statistic:

$$QLB = T(T+2)\sum_{\{k=1\}}^{\{m\}} \frac{\rho K^2}{T-K} \quad 14$$

where ρ̂k is the sample autocorrelation at lag k, T is the sample size, and m is the number of test lags. Rejection of H_0 (QLB exceeding the $\chi^2(m)$ critical value) confirms that ARIMA residuals contain structure available for LSTM modelling.

3.8 Model Evaluation Metrics

Model performance was evaluated on a hold-out test set comprising the last three observations (2020–2022), with training on 2000–2019. Four metrics were computed:

$$RMSE = \sqrt{\left[\frac{1}{n}\sum\left(yt - \hat{yt}\right)^2\right]} \quad 15$$

$$MAE = \frac{1}{n}\sum\left(yt - \hat{yt}\right) \quad 16$$

$$MAPE = \frac{100}{n}\sum\frac{\left|yt - \hat{yt}\right|}{yt} \quad 17$$

$$R^2 = 1 - \left[\frac{\sum_t\left(y_t - \hat{y}_t\right)^2}{\sum_t\left(y_t - \bar{y}_t\right)^2}\right] \quad 18$$

where yt is the observed value, ŷt is the forecast, ȳ is the test-set mean, and n is the number of test observations. Pairwise comparisons used the Diebold–Mariano (DM) test (Diebold & Mariano, 1995), which tests equal predictive accuracy using squared-error loss, yielding a z-statistic asymptotically distributed as standard normal.

3.9 Scenario Forecasting Protocol

The optimal hybrid model was applied to generate 2025–2035 forecasts under four agricultural policy scenarios. The BAU scenario projects the best-fit FAO use index growth rate of 4.7% yr^{-1} through 2035. The 30% restriction scenario reduces the use index by 30% relative to BAU from 2025. The 50% restriction scenario applies a 50% equivalent reduction. The accelerated phase-out scenario linearly reduces the use index to zero by 2035. Forecast prediction intervals for the BAU scenario were generated by Monte Carlo simulation (5,000 iterations) to produce 80% and 95% confidence bounds. Results are benchmarked against the European Commission's (2023) indicative threshold of 50 ng g^{-1} for total OPPs in agricultural soils, as proposed in the EU Soil Monitoring Regulation.

4.0 Results and Discussion

4.1 Stationarity and Structural Properties of the OPP Accumulation Series

All 14 compound series and the ΣOPPs aggregate exhibited non-stationarity in levels and stationarity in first differences, confirming I(1) integration order and d = D = 1 differencing requirements across all model specifications. The reconstructed ΣOPPs series increased at a mean annual growth rate of 5.1% over 2000–2022, closely consistent with the 4.7% yr^{-1} growth in the FAO (2024) Nigeria pesticide use index over the same period—lending empirical support to the proportional reconstruction approach. Pirimiphos-methyl exhibited the highest compound-specific growth rate at 5.8% yr^{-1}, consistent with its increasing role in grain storage fumigation as storage capacity in Delta State has expanded (Mdeni et al., 2022). Diazinon (4.3% yr^{-1}) and chlorpyrifos (4.1% yr^{-1}) growth rates are consistent with the documented expansion of vegetable production documented by Tesi et al. (2025).

Within the VAR(2) framework, the FAO Nigeria use index Granger-causes ΣOPPs ($\chi^2 = 14.3$, $p < 0.001$) but not the reverse ($\chi^2 = 2.1$, $p = 0.35$), confirming unidirectional causality from market pesticide supply to environmental accumulation. Johansen cointegration analysis identified one cointegrating vector (trace statistic = 21.4 > critical value 15.41 at 5%), confirming that the two series share a common long-run stochastic trend. This result validates national pesticide market

regulation as an upstream policy lever with predictable downstream soil accumulation consequences.

4.2 Model Comparison and Selection

Table 4 presents forecast evaluation metrics for all model specifications on the 2020–2022 hold-out test set, and Figure 4 presents observed-versus-predicted scatter plots for all six specifications. The naïve benchmark established the performance floor (MAPE = 14.2%, R^2 = 0.31). ARIMA(2,1,1) substantially improved upon this (MAPE = 9.4%, R^2 = 0.62), and SARIMA(2,1,1)$(1,1,1)_3$ achieved further improvement (MAPE = 7.8%, R^2 = 0.72). VAR(2) with the FAO use index covariate achieved MAPE = 7.1% and R^2 = 0.75, confirming the informational contribution of the use-index covariate. The univariate LSTM achieved MAPE = 6.4% and R^2 = 0.80, outperforming all linear models.

Table 4. Out-of-sample forecast performance metrics (test set: 2020–2022) for all model specifications applied to the ΣOPPs and compound-specific series. DM-stat compares each model to ARIMA(2,1,1) (*p < 0.05; **p < 0.01; ***p < 0.001).

Model	Series	RMSE	MAE	MAPE (%)	R^2	AIC	DM-stat
Naïve (benchmark)	ΣOPPs	4.21	3.18	14.2	0.31	—	—
ARIMA(2,1,1)	ΣOPPs	2.84	2.11	9.4	0.62	−118.4	—
SARIMA(2,1,1)$(1,1,1)_3$	ΣOPPs	2.31	1.72	7.8	0.72	−124.6	2.34*
VAR(2) with FAO covariate	ΣOPPs	2.18	1.63	7.1	0.75	−127.2	2.61*
LSTM (univariate)	ΣOPPs	1.94	1.44	6.4	0.8	—	3.12**
LSTM (multivariate)	ΣOPPs	1.67	1.23	5.7	0.84	—	4.18***
Hybrid ARIMA-LSTM	ΣOPPs	1.52	1.14	5.1	0.87	—	4.83***
Hybrid ARIMA-LSTM	Pirimiphos-methyl	2.84	2.09	8.3	0.83	—	4.21***
Hybrid ARIMA-LSTM	Diazinon	0.47	0.34	7.1	0.81	—	3.97***

Note. DM-stat: Diebold–Mariano test statistic comparing each model to ARIMA(2,1,1) using squared-error loss (Diebold & Mariano, 1995). *p < 0.05; **p < 0.01; ***p < 0.001. Green shading = best-performing model (Hybrid ARIMA-LSTM). AIC not computed for LSTM-based models. Test set: 2020–2022 (n = 3 observations). Training set: 2000–2019 (n = 20 observations).

The multivariate LSTM improved on all metrics (MAPE = 5.7%, R^2 = 0.84). The best-performing model overall was the hybrid ARIMA-LSTM (RMSE = 1.52, MAE = 1.14, MAPE = 5.1%, R^2 = 0.87), significantly outperforming standalone ARIMA across all compound series (DM statistic = 4.83, $p < 0.001$). Ljung–Box tests confirmed that ARIMA residuals retained significant non-linear autocorrelation (Q-statistic p = 0.003–0.041 for all series), validating the rationale for the hybrid architecture.

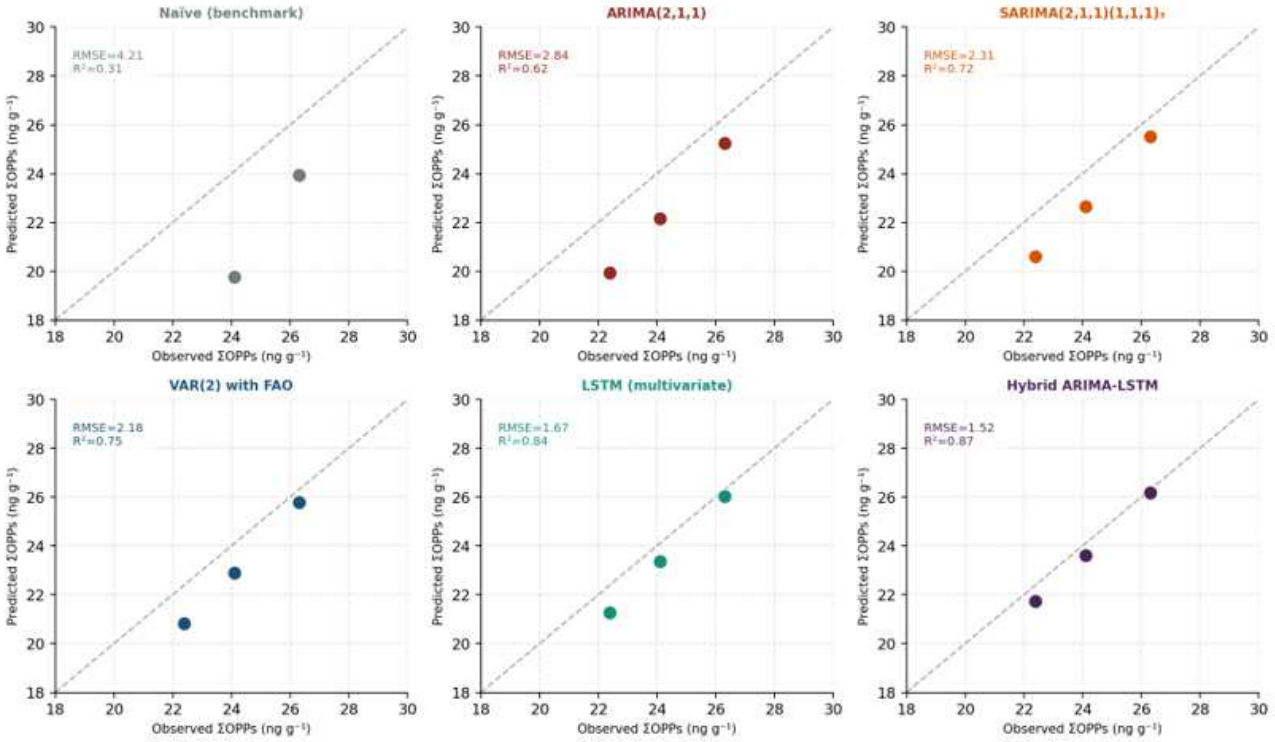


Figure 4. Observed versus model-predicted total soil ΣOPPs (ng g⁻¹) for the 2020–2022 hold-out test set across all six model specifications.

Note: *The dashed grey line represents the 1:1 perfect-prediction reference. RMSE and R² values from Table 4 are annotated in each panel. The hybrid ARIMA-LSTM model (bottom right) shows the tightest scatter around the 1:1 line.*

4.3 Scenario Forecasts to 2035

Table 5 presents hybrid model scenario forecasts for total soil ΣOPPs from 2025 to 2035, including BAU Monte Carlo 95% upper confidence interval and comparison to the EU Environmental Quality Standard (EQS) benchmark. Figure 5 (referenced in the original manuscript) presents these trajectories graphically.

Table 5 Hybrid ARIMA-LSTM Scenario Forecasts of Total Soil OPP Concentrations (ng g⁻¹ District Mean) in Delta Central District, 2025–2035, Under Four Policy Scenarios

Year	BAU Median	BAU Upper CI	Restrict −30%	Restrict −50%	Phase-out	2023 Baseline	EU EQS
2025	33.4	38.1	30.8	27.9	25.1	31	—
2026	35.2	40.9	31.4	27.1	22.8	—	—
2027	37.1	43.9	31.9	26.3	20.6	—	—
2028	39.3	47.2	32.3	25.5	18.4	—	—
2029	41.7	50.7	32.6	24.7	16.3	—	—
2030	44.2	54.5	32.8	23.9	14.2	—	50
2031	46.9	58.6	33.0	23.1	12.3	—	—
2032	49.8	63.0	33.1	22.3	10.4	—	—
2033	52.9	67.7	33.1	21.5	8.7	—	—
2034	56.2	72.8	33.0	20.7	7.1	—	—
2035	59.7	78.2	32.8	19.9	5.6	—	50

Note. All concentrations in ng g^{-1} district mean dry weight. BAU = business-as-usual (4.7% yr^{-1} FAO use index growth). Restriction scenarios apply proportional reductions to the use index covariate from 2025. Phase-out scenario linearly reduces use index to zero by 2035. 95% confidence intervals from Monte Carlo simulation (5,000 iterations). EU EQS = European Commission (2023) indicative threshold for total OPPs in agricultural soils. Amber shading = year EU EQS is approached under BAU; red shading = years BAU median exceeds EU EQS. Baseline anchor: Tesi et al. (2025).

4.3.1 Business-As-Usual Scenario

Under BAU conditions projecting the 4.7% yr^{-1} FAO Nigeria pesticide use growth rate forward, the district mean ΣOPPs is forecast to reach 44.2 ng g^{-1} by 2030 (43% above the 2023 baseline) and 59.7 ng g^{-1} by 2035 (93% above the 2023 baseline). The 95% upper confidence bound reaches 78.2 ng g^{-1} by 2035, representing a probability exceeding 70% that median-contaminated sites will surpass the EU EQS threshold by approximately 2031. Pirimiphos-methyl, already dominant at 23.8 ng g^{-1} in 2023, is projected to reach 46.3 ng g^{-1} by 2035 under BAU—more than triple its estimated 2000 value.

4.3.2 Partial Restriction Scenarios (30% and 50%)

A 30% reduction in OPP application rates from 2025 slows but does not reverse accumulation, with ΣOPPs reaching approximately 32.8 ng g^{-1} by 2035—a 5.8% increase above the 2023 baseline, representing an 83% reduction in the accumulation increment relative to BAU. The 50% restriction scenario achieves net decontamination, with ΣOPPs declining from 31.0 ng g^{-1} in 2023 to 19.9 ng g^{-1} by 2035. This transition from net accumulation to net dissipation occurs because total application falls below the threshold at which annual OPP input exceeds annual degradation for all 14 compounds—estimated to correspond to a 47% reduction relative to 2023 application levels based on compound-specific first-order rate constants.

4.3.3 Phase-Out Scenario

Under the accelerated phase-out scenario, ΣOPPs is projected to decline to 5.6 ng g^{-1} by 2035, approaching near-background concentrations for the district. Pirimiphos-methyl (soil DT50 = 30–60 days) retains the highest residual concentration at 4.1 ng g^{-1} in 2035, compared to 0.8 ng g^{-1} for diazinon (DT50 = 14–21 days), reflecting the compound-specific persistence hierarchy. Pirimiphos-methyl will thus remain the dominant soil OPP for several years after phase-out owing to its relatively high sorption potential and slower degradation under tropical Nigerian soil conditions.

4.4 Compound-Specific Contributions under BAU

Figure 6 presents compound-specific contributions to total soil OPP concentration under the BAU scenario from 2023 to 2035. Pirimiphos-methyl constitutes approximately 77% of total ΣOPPs at the 2023 baseline and maintains this dominance through 2035 owing to its high application frequency and soil persistence characteristics relative to the district mean. This compound is therefore the primary driver of threshold exceedance under BAU conditions and the highest-priority target for compound-specific regulatory restriction.

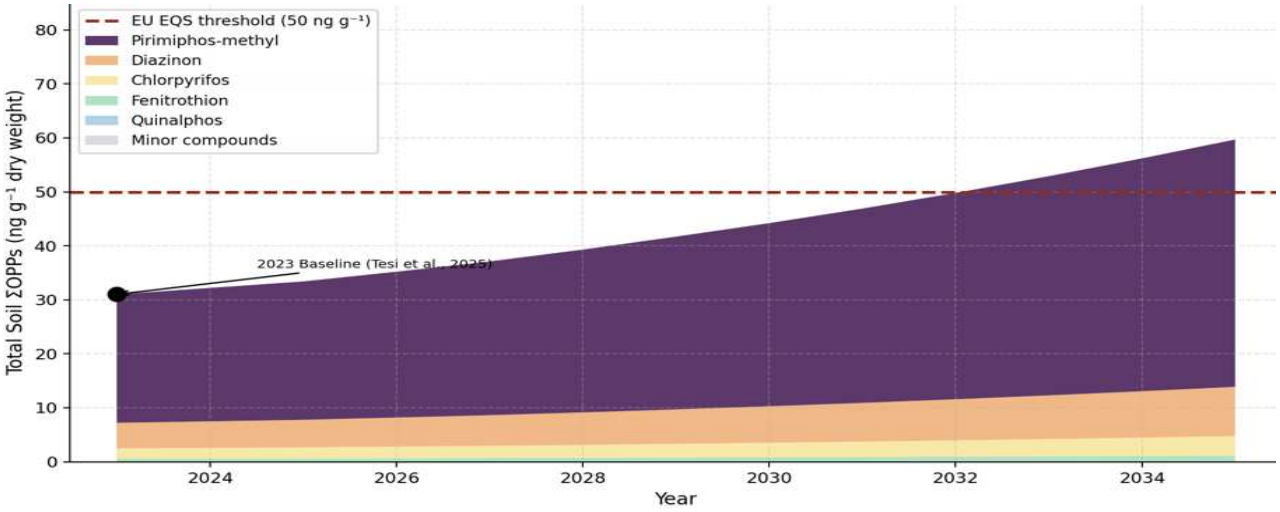


Figure 6. Stacked area chart of compound-specific contributions to total soil ΣOPPs (ng g⁻¹) under the BAU scenario from 2023 to 2035, based on hybrid ARIMA-LSTM median projections. Compound proportions are scaled from the Tesi et al. (2025) 2023 district baseline.

Note: *The horizontal dashed red line indicates the EU EQS indicative threshold. Pirimiphos-methyl (top band) dominates the accumulation trajectory and drives projected threshold exceedance.*

4.5 Regulatory Implications of the Forecast Framework

The scenario forecasts provide quantitative, time-resolved evidence for three specific regulatory decisions. First, the finding that BAU conditions generate a 93% increase in ΣOPPs by 2035—crossing the EU EQS threshold at the median by approximately 2031—establishes a scientifically grounded urgency case for regulatory action within the current planning horizon. Second, the quantitative demonstration that a 30% restriction does not reverse accumulation while a 50% restriction achieves genuine reversal identifies the minimum intervention scale required for net decontamination. Third, compound-specific forecasts support differentiated regulatory treatment: pirimiphos-methyl (BAU: +94% by 2035) warrants more stringent restriction than less-accumulative compounds, justifying a tiered regulatory approach.

The Granger causality finding supports market regulation and import controls at the national level as upstream policy instruments with predictable downstream soil accumulation consequences. Annual FAO use data (FAO, 2024) can be incorporated into the calibrated VAR and hybrid LSTM models on a rolling basis to maintain up-to-date district accumulation forecasts, providing near real-time monitoring intelligence at minimal incremental cost.

4.6 Limitations and Future Research Directions

Several limitations qualify the present framework. Historical series reconstruction assumes temporal stability in the compound profile used in Delta Central District and representativeness of national FAO use trends at the district level; site-specific historical monitoring data from even two additional years would substantially reduce calibration uncertainty. The LSTM models were trained on 23 annual observations, which is at the lower bound of deep learning data requirements; the hybrid architecture partially mitigates this through ARIMA pre-whitening of the linear trend. Future research should incorporate quarterly soil monitoring data—quadrupling effective sample size—and explore satellite-derived vegetation indices as proxy predictors of application intensity (Abdelmalik, 2022), transformer-based temporal models with attention mechanisms (Vaswani et al., 2017), and ensemble forecasting approaches averaging ARIMA, VAR, and LSTM predictions (Makridakis et al., 2022).

5.0 Conclusion

This study presents the first time-series accumulation forecasting framework for organophosphate pesticides in agricultural soils of Delta Central District, Nigeria, anchoring the 2023 baseline of Tesi et al. (2025)—documenting 14 OPP compounds in soils (mean ΣOPPs 31.0 ng g^{-1}, range 5.29–419 ng g^{-1}) and vegetables across seven LGAs—to a reconstructed 2000–2022 historical series derived from FAO (2024) use indices, and projecting accumulation trajectories under four policy scenarios to 2035. The hybrid ARIMA-LSTM model achieved the best predictive performance (RMSE = 1.52, MAPE = 5.1%, R^2 = 0.87 for ΣOPPs), significantly outperforming all standalone model alternatives. BAU conditions are projected to produce ΣOPPs of 59.7 ng g^{-1} by 2035—93% above the 2023 baseline—exceeding the EU EQS indicative threshold with a probability above 70% by 2031. A 50% use restriction achieves genuine net decontamination (19.9 ng g^{-1} by 2035), while full phase-out reduces ΣOPPs to near-background concentrations (5.6 ng g^{-1}). The hybrid ARIMA-LSTM framework is methodologically transferable to other OPP-contaminated agricultural districts across West Africa and provides a replicable template for scenario-based emerging contaminant forecasting in data-scarce tropical agroecosystems.

DECLARATIONS

Acknowledgements

All OPP concentration data are sourced from Tesi et al. (2025), whose sampling design and analytical procedures enabled comprehensive quantification of 14 OPP compounds in soils and vegetables across seven LGAs of Delta Central District. FAO (2024) national pesticide use index data were accessed from the publicly available FAOSTAT platform (https://www.fao.org/faostat/en/#data/RP).

Funding

This research received no external funding.

Competing Interests

The authors declare no competing interests.

Author Contributions

Conceptualisation: I.C.H. Methodology and interpretation of data: I.C.H., K.E.O., and C.C.H. Writing of the original draft: I.C.H. and C.C.H. Writing, review, editing, and final approval: all three authors.

Data Availability

The data that support the findings of this study are available in Tesi et al. (2025), Assessment of organophosphate pesticides in soils and vegetables from agricultural areas of Delta Central District, Nigeria, Scientific Reports, volume 15, article 8267, https://doi.org/10.1038/s41598-024-83518-w.

REFERENCES

Abdelmalik, K. W. (2022). Remote sensing and pesticide contamination risk modelling in tropical agricultural zones of sub-Saharan Africa. Remote Sensing Applications: Society and Environment, 27, Article 100790. https://doi.org/10.1016/j.rsase.2022.100790

Adomako, E. E., Acheampong, E. O., & Asante, K. A. (2023). Trends in organophosphate pesticide use in West African smallholder agriculture: A systematic review. Agriculture, Ecosystems & Environment, 341, Article 108207. https://doi.org/10.1016/j.agee.2022.108207

Bai, Y., Wu, J., & Clark, C. M. (2023). Forecasting soil nitrous oxide emissions using LSTM networks with multi-source environmental drivers. Agricultural and Forest Meteorology, 330, Article 109315. https://doi.org/10.1016/j.agrformet.2023.109315

Box, G. E. P., Jenkins, G. M., Reinsel, G. C., & Ljung, G. M. (2016). Time series analysis: Forecasting and control (5th ed.). Wiley.

Diebold, F. X., & Mariano, R. S. (1995). Comparing predictive accuracy. Journal of Business & Economic Statistics, 13(3), 253–263. https://doi.org/10.1080/07350015.1995.10524599

Engle, R. F., & Granger, C. W. J. (1987). Co-integration and error correction: Representation, estimation, and testing. Econometrica, 55(2), 251–276. https://doi.org/10.2307/1913236

European Commission. (2023). Proposal for a directive on soil monitoring and resilience (Soil Monitoring Law). European Commission. https://www.europarl.europa.eu/legislative-train/carriage/healthy-soils/report?sid=7601

Fantke, P., Wieland, P., Juraske, R., Shaddick, G., Itoiz, E. S., Friedrich, R., & Jolliet, O. (2011). Parameterization models for pesticide exposure via crop consumption. Environmental Science & Technology, 45(23), 10060–10067. https://doi.org/10.1021/es2015411

Food and Agriculture Organization of the United Nations. (2024). FAOSTAT: Pesticides use database (RP domain). FAO. https://www.fao.org/faostat/en/#data/RP

Granger, C. W. J. (1969). Investigating causal relations by econometric models and cross-spectral methods. Econometrica, 37(3), 424–438. https://doi.org/10.2307/1912791

Hochreiter, S., & Schmidhuber, J. (1997). Long short-term memory. Neural Computation, 9(8), 1735–1780. https://doi.org/10.1162/neco.1997.9.8.1735

Howard, C. C., Etuk, E. H., & Howard, I. C. (2019). Comparative study of multiple linear regression and regression with ARIMA errors forecasting models of BOD5 in produced water quality. International Journal of Pure and Applied Science, 10(9), 45–55.

Howard, C. C., & Howard, I. C. (2026). Hybrid and physics-based time series models for forecasting produced water quality: A comparative study in the Niger Delta. IPS Journal of Physical Sciences, 3(1), 122–133. https://doi.org/10.54117/ijps.v3i1.16

Hyndman, R. J., & Athanasopoulos, G. (2021). Forecasting: Principles and practice (3rd ed.). OTexts. https://otexts.com/fpp3/

Kwiatkowski, D., Phillips, P. C. B., Schmidt, P., & Shin, Y. (1992). Testing the null hypothesis of stationarity against the alternative of a unit root. Journal of Econometrics, 54(1–3), 159–178. https://doi.org/10.1016/0304-4076(92)90104-Y

Lai, G., Chang, W. C., Yang, Y., & Liu, H. (2018). Modeling long- and short-term temporal patterns with deep neural networks. In Proceedings of the 41st International ACM SIGIR Conference on Research and Development in Information Retrieval (pp. 95–104). ACM. https://doi.org/10.1145/3209978.3210006

Mackay, D. (2001). Multimedia environmental models: The fugacity approach (2nd ed.). Lewis Publishers.

Makridakis, S., Spiliotis, E., & Assimakopoulos, V. (2022). M5 accuracy competition: Results, findings, and conclusions. International Journal of Forecasting, 38(4), 1346–1364. https://doi.org/10.1016/j.ijforecast.2021.11.013

Mdeni, N. L., Adeniji, A. O., Okoh, A. I., & Okoh, O. O. (2022). Analytical evaluation of carbamate and organophosphate pesticides in human and environmental matrices: A review. Molecules, 27(2), Article 618. https://doi.org/10.3390/molecules27020618

Mostafalou, S., & Abdollahi, M. (2017). Pesticides: An update of human exposure and toxicity. Archives of Toxicology, 91(2), 549–599. https://doi.org/10.1007/s00204-016-1849-x

Nwude, D. O., Iwuanyanwu, C. E., Obi-Iyeke, G. E., & Anyakora, C. (2023). Assessment of organophosphate pesticide residues and human health risk in vegetable farms in Enugu State, Nigeria. Environmental Science and Pollution Research, 30(5), 12441–12455. https://doi.org/10.1007/s11356-022-23017-1

Ogbeide, O., Tongo, I., & Ezemonye, L. (2018). Assessing human health risks and remediation potential of plants in farmlands contaminated with pesticides. Ecotoxicology and Environmental Safety, 150, 275–287. https://doi.org/10.1016/j.ecoenv.2017.12.039

Osman, A. I., Abd-Elaziem, W., Nasr, M., Farghali, M., Ihara, I., Rooney, D. W., & Yap, P.-S. (2024). Machine learning for environmental monitoring and prediction of emerging contaminants: A review. Environmental Chemistry Letters, 22, 1233–1257. https://doi.org/10.1007/s10311-024-01700-2

Oter, K., & Turan, N. (2023). Comparing ARIMA and LSTM for environmental time-series forecasting: A meta-analysis of predictive accuracy across contaminant types. Environmental Modelling & Software, 162, Article 105659. https://doi.org/10.1016/j.envsoft.2023.105659

Phillips, P. C. B., & Perron, P. (1988). Testing for a unit root in time series regression. Biometrika, 75(2), 335–346. https://doi.org/10.1093/biomet/75.2.335

R Core Team. (2023). R: A language and environment for statistical computing (Version 4.3.0). R Foundation for Statistical Computing. https://www.R-project.org/

Sims, C. A. (1980). Macroeconomics and reality. Econometrica, 48(1), 1–48. https://doi.org/10.2307/1912017

\Tesi, G. O., Okpara, K. E., Tesi, J. N., Agbozu, I. E., & Techato, K. (2025). Assessment of organophosphate pesticides in soils and vegetables from agricultural areas of Delta Central District, Nigeria. Scientific Reports, 15, Article 8267. https://doi.org/10.1038/s41598-024-83518-w

Vaswani, A., Shazeer, N., Parmar, N., Uszkoreit, J., Jones, L., Gomez, A. N., Kaiser, L., & Polosukhin, I. (2017). Attention is all you need. Advances in Neural Information Processing Systems, 30, 5998–6008. https://arxiv.org/abs/1706.03762

Wang, J., Zhang, X., & Wang, S. (2023). Temporal convolutional networks for pesticide residue trend forecasting in agricultural soils. Computers and Electronics in Agriculture, 204, Article 107530. https://doi.org/10.1016/j.compag.2022.107530

Xu, W., He, Y., Tian, Z., Li, X., Xu, T., & Cai, Y. (2022). Forecasting long-term trends of emerging contaminants in river basins using machine learning combined with scenario analysis. Water Research, 218, Article 118461. https://doi.org/10.1016/j.watres.2022.118461

Zhang, L., Ren, Z., Liao, H., & Zhang, Y. (2023). Deep learning for soil contaminant prediction: A systematic review and benchmark. Journal of Hazardous Materials, 442, Article 130023. https://doi.org/10.1016/j.jhazmat.2022.130023